Title: Iron Regulatory Protein 1 is Required for the Propagation of Inflammation in Inflammatory Bowel Disease

Authors: L. Fahoum[1]†, S. Belisowski[1]†, N. Ghatpande[1], N. Guttmann-Raviv[1], W. Zhang[2], K. Li[2], W-H. Tong[3] A. Nyska[4], M. Waterman[5], R. Weisshof[5], A. Zuckerman[6], E.G. Meyron-Holtz[1*]

Affiliations:

[1]Laboratory of Molecular Nutrition, Department of Biotechnology and Food Engineering, Technion– Israel Institute of Technology, Haifa, Israel.

[2]Jiangsu Key Laboratory of Molecular Medicine, Medical School of Nanjing University, Nanjing 210093, China

[3]Molecular Medicine Program, Eunice Kennedy Shriver National Institute of Child Health and Human Development, Bethesda, MD 20892, USA

[4]Tel Aviv University and Consultant in Toxicologic Pathology, Tel Aviv, Israel.

[5]Rambam / Technion– Israel Institute of Technology, Haifa, Israel.

[6]Aviv Projects, Ness Ziona, Israel.

*Corresponding author. Email: Meyron@technion.ac.il
†These authors both contributed most significantly to this work

Abstract:

Inflammatory bowel diseases (IBD) are complex disorders characterized by a cycle of inflammatory perpetuation. Iron accumulates in the inflamed tissue of IBD patients, yet neither a mechanism for the accumulation nor its implication on the course of inflammation are known. This study addresses the role of iron homeostasis in IBD using human biopsies, animal models and cellular systems. It demonstrates inflammation-mediated modifications of iron homeostasis, and an iron decoupled activation of the iron regulatory protein (IRP)1. To understand the role of IRP1 in the course of this inflammation-associated iron pattern, a novel cellular co-culture model was established, that reproduced the iron-pattern observed *in vivo.* Importantly, deletion of IRP1 from an IBD mouse model completely abolished mis-distribution of iron and intestinal inflammation, suggesting a central role of IRP1 in the coordination of inflammatory response in the intestinal mucosa. Thus, this work identifies IRP1 as a target for IBD treatment.

One-Sentence Summary: We show that a miss regulated iron homeostasis mediates the exacerbation of the inflammation in inflammatory bowel diseases.

Introduction

IBDs are long-term multifactorial inflammations of the gastrointestinal tract with increasing global prevalence (*1*). Although the cellular and molecular events initiating and perpetuating the inflammation are not fully understood, it is clear, that intestinal homeostasis is broadly disrupted, causing pathological inflammation that leads to tissue injury. Iron accumulation has been noticed in the inflamed tissues of CD and colitis patients (the two most prevalent forms of IBD), compared to non-inflamed areas of the same patients and of healthy individuals (*2*), but neither the role nor the mechanism of this phenomenon is known.

Iron is an essential nutrient, yet unbalanced iron levels lead to inflammation and tissue damage (*3-5*). Iron homeostasis is tightly regulated, at the systemic and cellular level, primarily by the peptide hormone hepcidin (*6*) and by the iron regulatory proteins (IRP) 1 and 2 respectively (*7*). Hepcidin binds to the iron exporter ferroportin, sterically inhibits iron export and causes ferroportin degradation (*8*) (*9*). IRPs regulate numerous transcripts, mostly related to cellular iron import, storage and export, by binding with high affinity to RNA motifs known as iron-responsive elements (IREs). IREs are found in the 5' or 3' UTR of mRNAs. Ferritin is a 24-subunit multimer, composed of two kinds of subunits FTH1 and FTL (*10-12*). Transcripts of both subunits contain a 5' IRE and translation is inhibited by active IRPs. The ratio of the subunits differs in various cell types and pathophysiological conditions, due to transcriptional modifications (*13*). In contrast the iron importer transferrin receptor, (TFR1) has IREs in the 3' UTR, and IRP-IRE binding stabilizes the transcript, leading to increased iron import. The two IRPs each sense and respond to cytosolic iron and oxygen (and reactive oxygen- and nitrogen- species (ROS/RNS)) in their own specific ways (*14*). IRP1 is a bifunctional protein that changes its conformation from a cytosolic iron-sulfur cluster containing aconitase (cAco) to an RNA (IRE)-binding apoprotein. At physiologic oxygen conditions, the Fe-S cluster of cAco is relatively stable and IRP1 does not change to its RNA-binding form, even when iron levels are low (*15-17*). In contrast, IRP2 is degraded in the presence of high iron, oxygen and ROS/RNS levels (*18*), yet maintains its ability to respond to cellular iron levels over a wide range of oxygen concentrations (*19*).

Although IRP1 and IRP2 were first identified as iron-sensors that mediate the regulation of iron homeostasis, studies on inflammation have shown changes in iron homeostasis in macrophages that were mediated by IRP response to nitric oxide (NO). NO is a gaseous signaling molecule that plays important roles in pathogen killing, as well as macrophage metabolic and epigenetic remodeling (*20*). NO, produced by macrophages, diffuses into proximal cells, allowing for temporally and spatially complex signaling dynamics in tissues (*21*). Dysregulation of IRP1 and IRP2 has been observed in patients with genetic hemochromatosis and was attributed to the release of NO produced in activated macrophages (*22, 23*). The opposing biological consequences of NO mediated IRP1 activation versus IRP2 degradation on cellular iron, TfR1 and ferritin, was extensively studied in macrophages (*23-25*), yet in the systemic context of specific inflammatory diseases they remain unclear.

Here, using human biopsies of CD patients, animal models for CD and colitis and a cellular co-culture model that mimics the interaction between intestinal epithelium and -immune cells, we studied the inflammatory iron homeostasis in IBD. We found that IRP1 is activated by the inflammation, that this activation mediates an inflammatory regulation of iron homeostasis and participates in the propagation of inflammation in IBD. Most importantly, targeted deletion of IRP1 minimizes the inflammation, making it a novel target for the treatment of IBD.

Results

IRP1 activation is inconsistent with a newly identified inflammatory iron pattern in IBD mouse models.

To evaluate the effect of inflammation on iron homeostasis and IRP activity in vivo, we used a genetic mouse model for CD, the tumor necrosis factor alpha-overexpressing mice (*Tnf*$^{\Delta ARE/+}$) and the chemical DSS model for colitis (*26*). *Tnf*$^{\Delta ARE/+}$ mice develop spontaneous inflammation in the terminal ileum at the age of 12-14 weeks and rheumatoid arthritis later in life (*27*). Intestinal sections of *Tnf*$^{\Delta ARE/+}$mice were stained for ferritin, a sensitive indicator of cellular iron status (*10*). Ferritin accumulated in the immune cells, and was significantly reduced in intestinal epithelial cells (IECs) of the inflamed terminal ileum of *Tnf*$^{\Delta ARE/+}$mice compared to wild-type (WT) controls (Fig. 1A, Fig.S1A). Similar results were obtained in sections from mice with DSS induced colitis (Fig. 1A, Fig. S1A). These observations suggested that the inflammation in these tissues caused a unique pattern of iron distribution, involving iron accumulation in the immune cells and iron deficiency in the IECs. To test if other iron-related proteins respond similarly, an IEC- and immune cell-enriched (lamina propria-LP) fraction was prepared from the terminal ileum of *Tnf*$^{\Delta ARE/+}$ mice and various proteins, known to respond to cellular iron levels, were analyzed. Consistent with the inflammatory ferritin-response, IEC-TFR1 levels were increased and LP-TFR1 levels reduced, when compared to the WT fractions (Fig.1B), supporting the modified iron pattern discovered in these two cell fractions. In addition, IRP2, which similarly to TFR1, is elevated in iron deprivation (*28, 29*), was increased in the inflamed IECs and decreased in the inflamed LP (Fig. 1C). However, IRP1-IRE-binding activity, which was assessed via electromobility shift assay (EMSA), was significantly elevated in both fractions of the inflamed ileum compared to WT. This result suggested, that the regulation of IRP1 activity is independent of the intracellular iron state (Fig. 1D).

In a cell-culture model, physical contact is required between macrophages and epithelial cells, to mimic the inflammatory regulation of iron homeostasis

To elucidate what drives the iron independent activation of IRP1 and the intestinal inflammatory iron pattern observed in mice, we searched for a suitable cell-model. Several co-culture models of epithelial cells (EC) with immune cells, that use filter inserts have been successfully employed to reproduce various aspects of inflammation (*30-32*), yet none of these models could reproduce the inflammatory iron pattern. We hypothesized that NO produced by macrophages diffuses and activates IRP1 in neighboring ECs, and that this activation mediates the inflammatory iron pattern. Thus, we tested co-cultures with direct cell-to-cell contact between ECs and macrophages. To differentiate between proteins such as IRP1, IRP2, ferritin and TfR1 in the ECs and the macrophages, we developed co-cultures of the human epithelial enterocyte-like Caco2 cells, with either murine primary bone marrow-derived macrophages (BMDM) or the murine macrophage-like cell line Raw 264.7 (*33*). Lipopolysaccharide (LPS) was applied to elicit inflammation, which was validated by the activation of key markers of signaling pathways involved in inflammation, including MAP kinase pathways and NFkB-p65 (Fig. S2A). In addition, downstream proinflammatory cytokines, including *Il8* and *Icam1* in ECs (Fig. S2B) and *Tnfα*, *Icam1*, *Il1b* and *Il6* in macrophages (Fig. S2C), were all activated in both co-cultures and the time-course of the LPS-triggered inflammatory response was nearly identical to that reported for *in vivo* and *in vitro* models of LPS induced inflammation (*34-36*).

The LPS-triggered response was identified in both, macrophage mono-cultures and macrophage-EC co-cultures, but not in EC mono-cultures (Fig. S3A), further supporting the necessity of macrophage vicinity for the epithelial inflammatory response. Significantly, the NO donor S-nitro-

N-acetyl-D, L-penicillamine (SNAP) elicited an inflammatory response in EC monocultures (Fig. S3B). Further, in SNAP-treated ECs, intracellular iron was reduced and extracellular iron increased (Fig. S3C), supporting the notion that NO generated in macrophages (Fig S3A) diffuses to the ECs in the co-cultures and that NO contributes to the inflammatory iron pattern.

To assess whether LPS-induction of inflammation in the co-cultures follows the *in vivo* pattern of modified iron homeostasis in the two cell populations, the RNA-binding activity of IRP1 was determined by EMSA. Due to slight differences in molecular weight between human and mouse proteins as well as the primer specificity to human or mouse genes, protein- and mRNA- levels from each cell type could be distinguished. Indeed, RNA binding activity of macrophage IRP1 was significantly increased after LPS stimulation (Fig. 2A lane 3 and 4), similar to the observation in the *Tnf*$^{\Delta ARE/+}$ mice (Fig. 1D). Yet, epithelial IRP1 could not be similarly evaluated, as it migrated together with macrophage IRP2. Therefore, IRP1 aconitase activity was evaluated using the in-gel aconitase-assay, as decreased cAco-aconitase-activity correlates with increased IRP1 RNA-binding-activity (*37*). Gel conditions were optimized to enable differentiation of human from mouse cAco-aconitase-activity in ECs and macrophages (Fig. 2B lane 1 and 4). A decrease in cAco activity in response to LPS treatment was observed in both cell types, which is consistent with an increase in the RNA-binding-activity of IRP1. Moreover, LPS treatment led to a significant decrease in mitochondrial aconitase (mAco) activity in both cell types, suggesting a metabolic shift to glycolysis, as previously reported (*38, 39*). Taken together, we developed a direct interspecies co-culture model, that upon induction of inflammation with LPS, activated a broad range of inflammatory signaling pathways. Most importantly the cell-model mimicked the inflammatory iron pattern and the increased IRP1 mRNA-binding activity in both, ECs and macrophages as seen in vivo (Fig.1D).

Inflammatory pathways support the activation of IRP1-IRE binding activity

To further elucidate the mechanism driving the increased IRP1-IRE-binding activity in each cell type, and considering that Fe-S cluster assembly proteins Nfs1 and IscU mRNA and protein levels were reported to be low in BMDM in response to inflammation (*40*), several genes involved in Fe-S cluster assembly were evaluated. In macrophages, the transcription levels of all four tested iron-sulfur cluster biogenesis proteins were significantly decreased, in agreement with the decrease in aconitase activities in mAco and cAco. However, in epithelial cells, transcripts of iron-sulfur cluster biogenesis proteins did not change (Fig. 2C). In IBD, the epithelial transcription regulator HIF2α is increased (*41*), and given that HIF2α is a key regulator of iron transport through epithelial cells (*42*), cytosolic and nuclear HIF2α levels were assessed and found to be significantly increased, beginning 4h after LPS stimulation (Fig. 2D). In line with this, 4h after LPS stimulation levels of both the apical iron importer DMT1 and the basolateral iron exporter FPN gradually increased (Fig. S4), likely promoting increased iron flux through the epithelial cells. This can explain the observed epithelial iron deficiency and consequential increase in IRP1 RNA-binding activity. Altogether, increased NO production, decreased iron-sulfur cluster assembly proteins and increased HIF2α support the inflammatory activation of IRP1-IRE binding activity in both, macrophages and epithelial cells. Next, we tested the response of IRP regulated genes, to the increased IRP1-activity.

Increased IRP1-activity mediates changes in TfR1 and ferritin levels and ferritin subunit composition

To test the effect of inflammation-mediated modifications of IRP-activity on iron status and IRP-regulated proteins in the co-culture, we analyzed changes in ferritin-iron content upon LPS-stimulation. Epithelial ferritin iron was reduced and macrophage ferritin iron was elevated 24 hr after LPS-stimulation (Fig. 3A lanes 10 and 11), suggesting that similarly to the observation *in vivo*, epithelial cells of the co-culture take on an iron-deficiency phenotype, while macrophages take on an iron-loaded phenotype. In addition, a strong increase in macrophage ferritin protein, especially of the FTH1 subunit, was detected in the co-cultures (Fig. 3B), consistent with the observations in macrophage mono-cultures (*43*). Considering the activation of IRP1, and thus inhibition of ferritin translation, we thought that the ferritin increase in macrophages could be due to an inflammation-mediated decrease in ferritin degradation. Pulse-chase analysis of co-cultures that were metabolically labeled with ^{35}S just before stimulation with LPS showed that macrophage ferritin subunit-degradation was slower in LPS-treated co-cultures (Fig. 3C lane 9 and 11), compared to untreated controls (Fig. 3C lane 8 and 10). A decrease in ferritin degradation was further suggested by a decrease in transcript levels of the ferritinophagy-mediating *Ncoa4* in the inflamed BMDM (Fig. 3D). After 24 hr of LPS stimulation, macrophage ferritin migrated slightly faster in the native gel (Fig. 3A lane 11), compared to its non-treated counterpart (Fig. 3A lane 10), suggesting a shift in subunit composition of ferritin towards H-rich heteropolymers (Fig. S5A). Indeed, the transcript levels of *Fth1* were markedly increased after LPS stimulation, whereas transcript levels of *Ftl* remained relatively unchanged (Fig. S5B). A similar increase of FTH1 was reported in monocytes exposed to inflammatory conditions (*44*). In agreement, the FTH1:FTL protein ratio shifted from approximately 1:1 in the control macrophages to around 3:1 after LPS stimulation (Fig. S5C). In epithelial cells in contrast, LPS stimulation led only to a slight increase in *Fth1* transcript-levels, alongside a significant increase in *Ftl* transcript levels (Fig. S5B). Nevertheless, epithelial ferritin protein concentration remained below detectable levels in immunoblots; only epithelial ferritin-iron could be detected and this was decreased after 24 hr of LPS stimulation, as mentioned above (Fig 3A). In summary, the complex dynamics of ferritin synthesis and degradation during inflammation led to an increase in macrophage ferritin and ferritin-iron, and a decrease in epithelial ferritin-iron, in agreement with the observations in the inflamed lesion of $Tnf^{\Delta ARE/+}$mice (Fig. 1A).

To further validate the observed inflammatory iron pattern in the epithelial-macrophage co-culture, changes in mRNA levels of the iron importer TFR1 were evaluated following LPS induction (Fig.3E). We found that *Tfr1* mRNA levels decreased in the macrophages and increased in the Caco2 cells 24 hr after LPS exposure, consistent with the iron accumulation in the macrophages and the iron decrease in the IECs of the $Tnf^{\Delta ARE/+}$ mice. The *Tfr1* mRNA decrease in macrophages was preceded by an increase in *Tfr1* transcripts, identified 2h after LPS stimulation, suggesting an early inflammation-mediated increase in iron import that contributes to iron accumulation in the macrophages (Fig.3E). Protein levels of TFR1 could be differentially analyzed for epithelium and macrophages, due to the slight differences in the migration of human and mouse TFR1 in SDS-PAGE. 24 hr after LPS stimulation, TFR1 protein was increased in the epithelium and decreased in macrophages, aligning with the differential iron status of the two cell types (Fig.3F).

Taken together, in epithelial cells, the decrease in ferritin and increase in TFR1 are in line with the activation of IRP1. In the macrophages however, where high iron makes us expect low IRP1-RNA-binding activity, the IRP1 activation was decoupled from cellular iron status, and ferritin and TFR1 regulation were dominated by the iron loaded phenotype.

IRP1-activity mediates the inflammatory iron homeostasis and contributes to the propagation of inflammation

Since IRP1 RNA-binding activity was increased in inflamed macrophages, regardless of their iron-loaded phenotype (Fig. 1-3), we hypothesized that this activation may play a role in the course of the inflammation. Thus, the effect of IRP1 knockout in macrophages on inflammatory markers was assessed. The classical inflammatory response of the co-culture with *Irp1*$^{-/-}$ macrophages was reminiscent of the co-cultures with WT macrophages in all inflammatory parameters tested, including the levels of secreted epithelial cytokine IL8 and transcript levels of the macrophage inflammation markers *Tnfα, Icam1* and *Il6* (Fig.S6A and B). In parallel, levels of the macrophage inflammatory mediator NO in the medium of both co-cultures were similarly increased in response to LPS stimulation (Fig. S6C). Next, the effect of IRP1 knockout in macrophages on the inflammatory iron pattern was assessed. Co-cultures of WT-epithelial cells with either IRP1$^{-/-}$- or WT macrophages responded similarly to LPS stimulation. Specifically, FTH1 was significantly increased in macrophages of both genotypes in inflamed co-cultures (Fig.4A). Further, aconitase activities were significantly decreased in both co-cultures (Fig.4B), indicating that deletion of IRP1 in the macrophages alone did not reverse the inflammatory changes in iron-homeostasis. Taken together, these results suggest that the noncanonical activation of macrophage-IRP1 is not solely responsible for the generation of the inflammatory iron pattern. As epithelial cells have been shown to play a critical role in the pathophysiology of IBD (*45*, *46*), and epithelial iron deficiency has been associated with an inflammatory response (*47*), the effect of epithelial IRP1 activation on the inflammation was assessed. To this end, IRP1 was activated by addition of a stable aminoxyl radical Tempol, to the co-culture (*48*). LPS stimulation, of co-cultures with Tempol pretreated epithelial cells, elicited a greater inflammatory response in the epithelial cells compared to epithelial cells in co-cultures without Tempol pretreatment (Fig. 4C). Without LPS stimulation, tempol treatment alone did not elicit a significant inflammatory response in the co-cultures (Fig.S6D). These results suggested that epithelial IRP1 contributes to the course of the inflammation. Thus, we tested whether IRP1 also contributes to the course of inflammation *in vivo*. To do this, a targeted deletion of IRP1 was introduced to *Tnf*$^{\Delta ARE/+}$ mice. To visualize iron in the terminal ileum sections, systemic iron overload was necessary. The systemic iron overload did not affect the histological inflammation score (Fig S7A). Ferric iron levels in iron-loaded mice were significantly increased in the lamina propria of the terminal ileum of *Tnf*$^{\Delta ARE/+}$ mice compared to WT mice, whereas in terminal ileum sections of the of *Tnf*$^{\Delta ARE/+,Irp1\text{-}/\text{-}}$ mice iron levels resembled the level of non-inflammatory WT mice (Fig.5A). This suggested that the deletion of IRP1 may also result in a reduction in intestinal inflammation. Indeed, *Tnf*$^{\Delta ARE/+,Irp1\text{-}/\text{-}}$ mice showed no signs of histologically assessed inflammation (Fig. 5B-C). Furthermore, the pro-inflammatory response was significantly minimized, as indicated by reduced *Tnfα* and *Icam1* levels (Fig. 5D). These results indicated that the activation of IRP1-RNA binding activity is required for the propagation of the terminal ileum inflammation in *Tnf*$^{\Delta ARE/+}$ mice.

Modified iron homeostasis is observed in the inflamed lesions of CD patients

Finally, to evaluate if the iron homeostasis in CD patients is modified by the inflammation in a similar manner as observed in the mouse- and cell-models, we labeled sections of intestinal biopsies from CD patients for ferritin by IF. Comparing inflamed to non-inflamed sections from the same patients, we found that ferritin levels were significantly reduced in IECs of inflamed, compared to non-inflamed areas from the same patients (Fig. 6A, Fig. S7B).

In summary, we found an inflammation-mediated activation of IRP1, that in macrophages is decoupled from the cellular iron level. IRP1 activation modifies iron homeostasis to an inflammatory iron pattern that includes a decrease in epithelial- and an increase in macrophage-

iron. We detected this modified iron-pattern in human biopsies from CD-patients, and in mouse models for CD and colitis and we were able to mimic it in cellular co-cultures. Targeted deletion of IRP1 in *Tnf*$^{\Delta ARE/+}$ mice completely reversed the inflammatory iron pattern and no inflammation was detected, despite the genetically engineered overexpression of TNFα in these mice.

Discussion

Inflammation is a response to structural or functional insults, and also an integral part of animal physiology, particularly as a means to correct homeostatic instability (*49*). Both genetic and environmental factors contribute to the development of IBD, yet what triggers the inflammatory process that is characterized by modifications of the intestinal microbiota, impaired intestinal barrier function and the recruitment of the immune system, remains unclear. It is known though, that early on in the process, local immune cells are activated and secrete nitric oxide, other proinflammatory molecules and cytokines (*50*).

The present work shows that cellular iron homeostasis is modulated in IBD. We show a pathological iron distribution manifested by decreased iron stores in IECs and increased iron stores in LP macrophages. This establishes a homeostatic instability that eventually perpetuates an inflammatory process, as both increased and decreased iron levels were shown to mediate inflammation (*3-5*). Our work suggests, that the inflammation-associated iron pattern was driven by the activation of IRP1. Similarly, in a model of non-alcoholic fatty liver disease, elevated IRP1 RNA-binding-activity was found on the background of high iron in rat livers (*51*), demonstrating activation of IRP1 in an inflammatory context, decoupled from iron status. In IBD, increased ROS/RNS release from activated macrophages and reduced cluster assembly can explain the IRP1 activation (*24*, *52*, *53*). Our results demonstrated iron decoupled activation of IRP1 in macrophages, and suggest that this activation signals a pseudo-iron deficiency, contributing to further iron influx. Increased iron-levels were shown to promote a proinflammatory phenotype of macrophages (*5*).

In epithelial cells, HIF2α was activated (Fig 2D.), in line with activated NFkB-p65 eliciting the activation of HIF2α (*54*). HIF2α activation is possibly further supported by NO mediated iron efflux (*55*) that leads to prolyl-hydroxylase deactivation (*56*). HIF2α activation induces an increased iron flux that includes iron import through the apical membrane and iron export from the basolateral membrane, securing the repletion of body iron levels in iron deficiency (*57*). This increased iron flux may further contribute to the reduced iron levels in the epithelial cells and the activation of IRP1. In addition, drug induced activation of IRP1 in epithelial cells, increased the production of proinflammatory cytokines by these cells (Fig. 4D). Thus, the activation of IRP1 RNA binding activity plays a role in the establishment of an inflammatory iron-homeostasis that supports the exacerbation of the inflammatory process, as summarized in a cartoon in figure 6B. This model is supported by our key finding that deletion of IRP1 abolished the inflammation of the *Tnfα* overexpressing mice (Fig. 5A-D). An inflammation-driven regulation of iron homeostasis is thus a factor that plays an active role in the series of events that contribute to the course of inflammation.

Direct interference with systemic iron levels, by administering a low iron diet, can reduce inflammation in *Tnf*$^{\Delta ARE/+}$ mice (*58*). Local regulation of iron homeostasis was also demonstrated to play an important role in the pathophysiology of IBD. For example, hepcidin, which is generally regarded as a systemic iron regulator and is locally produced by conventional dendritic cells in the colon, regulates luminal iron content and supports local tissue repair (*59*). Further, the pathophysiology of IBD is closely connected to the microbial homeostasis of the gut. Decreased

iron content in the intestinal lumen triggers lactobacillus-mediated reduction of iron uptake by decreasing HIF2α activity (*60*), thus possibly connecting the microbial composition also with epithelial IRP1 activity.

Our data of opposing inflammatory regulation of iron homeostasis, that included iron increase in macrophages and iron decrease in epithelial cells in the same tissue, complicated studying mechanisms that drive this redistribution of iron. We therefore looked for a cellular co-culture system featuring the same inflammation-associated iron pattern. Upon activation, many of the published co-culture setups mimicked well-established inflammatory parameters, however did not replicate the inflammatory iron pattern (unpublished data). We showed, that the inflammatory iron homeostasis was only established, when epithelial cells and macrophages were in direct contact. The cell-to-cell contact enabled us to mimic the same iron and ferritin distribution in cell-cultures, that we observed in the $Tnf^{\Delta ARE/+}$ and DSS mouse models and the IBD patients. Inter-species co-cultures of Caco2 cells and Raw264.7 cells were successfully used to analyze inflammatory pathways (*33*) and human grafts of fetal intestine in SCID mice were used to study fistulae in IBD (*61*), supporting the functionality of human-mouse interspecies systems. The use of interspecies co-cultures had many advantages, especially, as it enabled differential analysis of iron-related proteins such as TFR1 and IRP1 from epithelial and macrophage origin. Using this model, we found that in response to the induction of inflammation, TFR1 was regulated by the iron status of the specific cell types (increased in epithelial cells and decreased in macrophages), as seen in the $Tnf^{\Delta ARE/+}$ animal-model. The interspecies co-culture also enabled analysis of inflammation-mediated changes in ferritin. In the macrophages, a significant increase in both ferritin-protein and ferritin-iron was measured in response to inflammation, as well as a significant shift in the ferritin subunit composition. In light of the recent findings that ferritin-NCOA4 complexes generate liquid-phase condensates (*62, 63*), and the specificity of NCOA4 for the H-subunit of ferritin (*64*), the change in subunit composition may have important implications on ferritin trafficking and tissue iron distribution.

Taken together, the presented findings demonstrate that an inflammation-induced shift in the regulation of cellular iron homeostasis is mediated by the activation of IRP1, and that this shift plays an active role in the propagation of inflammation in IBD. Reduction of IRP1 protein and activity in the non-inflammatory setting of superoxide dismutase 1 knock-out mice was previously reported to have no effect on iron homeostasis (*65*). However, when IRP1 is activated by inflammatory signals, it turns into a dominant regulator of iron homeostasis of inflammation. This is in contrast to the physiologic, non-inflamed state, where IRP2 plays a dominant role in iron regulation (*16, 19*). The interspecies co-culture model developed here, facilitated the analysis of interactions between intestinal epithelium and macrophages during inflammation and of the molecular details of the inflammation-associated iron pattern. Finally, correction of the iron homeostasis by interfering with IRP1 activity, halted the self-perpetuation of the inflammation. Thus, IRP1 may serve as a target for the treatment of IBD, inhibiting a pathway that is not directly involved in the immune system and may be manipulable with minimal side effects.

References

1. G. G. Kaplan, J. W. Windsor, The four epidemiological stages in the global evolution of inflammatory bowel disease. *Nature reviews. Gastroenterology & hepatology* **18**, 56-66 (2021).
2. L. Lih-Brody *et al.*, Increased oxidative stress and decreased antioxidant defenses in mucosa of inflammatory bowel disease. *Digestive diseases and sciences* **41**, 2078-2086 (1996).
3. Y. Yu, D. R. Richardson, Cellular iron depletion stimulates the JNK and p38 MAPK signaling transduction pathways, dissociation of ASK1-thioredoxin, and activation of ASK1. *The Journal of biological chemistry* **286**, 15413-15427 (2011).
4. A. U. Steinbicker, M. U. Muckenthaler, Out of balance--systemic iron homeostasis in iron-related disorders. *Nutrients* **5**, 3034-3061 (2013).
5. A. Kroner *et al.*, TNF and increased intracellular iron alter macrophage polarization to a detrimental M1 phenotype in the injured spinal cord. *Neuron* **83**, 1098-1116 (2014).
6. T. Ganz, E. Nemeth, Hepcidin and iron homeostasis. *Biochimica et biophysica acta* **1823**, 1434-1443 (2012).
7. N. Wilkinson, K. Pantopoulos, The IRP/IRE system in vivo: insights from mouse models. *Frontiers in pharmacology* **5**, 176 (2014).
8. S. Aschemeyer *et al.*, Structure-function analysis of ferroportin defines the binding site and an alternative mechanism of action of hepcidin. *Blood* **131**, 899-910 (2018).
9. E. Nemeth *et al.*, Hepcidin regulates cellular iron efflux by binding to ferroportin and inducing its internalization. *Science (New York, N.Y* **306**, 2090-2093 (2004).
10. P. M. Harrison, P. Arosio, The ferritins: molecular properties, iron storage function and cellular regulation. *Biochimica et biophysica acta* **1275**, 161-203 (1996).
11. E. W. Müllner, B. Neupert, L. C. Kühn, A specific mRNA binding factor regulates the iron-dependent stability of cytoplasmic transferrin receptor mRNA. *Cell* **58**, 373-382 (1989).
12. J. B. Harford, R. D. Klausner, Coordinate post-transcriptional regulation of ferritin and transferrin receptor expression: the role of regulated RNA-protein interaction. *Enzyme* **44**, 28-41 (1990).
13. F. M. Torti, S. V. Torti, Regulation of ferritin genes and protein. *Blood* **99**, 3505-3516 (2002).
14. M. U. Muckenthaler, B. Galy, M. W. Hentze, Systemic iron homeostasis and the iron-responsive element/iron-regulatory protein (IRE/IRP) regulatory network. *Annual review of nutrition* **28**, 197-213 (2008).
15. L. C. Kühn, Iron regulatory proteins and their role in controlling iron metabolism. *Metallomics* **7**, 232-243 (2015).
16. E. G. Meyron-Holtz *et al.*, Genetic ablations of iron regulatory proteins 1 and 2 reveal why iron regulatory protein 2 dominates iron homeostasis. *The EMBO journal* **23**, 386-395 (2004).
17. B. D. Schneider, E. A. Leibold, Effects of iron regulatory protein regulation on iron homeostasis during hypoxia. *Blood* **102**, 3404-3411 (2003).
18. E. S. Hanson, E. A. Leibold, Regulation of the iron regulatory proteins by reactive nitrogen and oxygen species. *Gene Expr* **7**, 367-376 (1999).
19. E. G. Meyron-Holtz, M. C. Ghosh, T. A. Rouault, Mammalian tissue oxygen levels modulate iron-regulatory protein activities in vivo. *Science (New York, N.Y* **306**, 2087-2090 (2004).
20. G. Natoli, F. Pileri, F. Gualdrini, S. Ghisletti, Integration of transcriptional and metabolic control in macrophage activation. *EMBO reports* **22**, e53251 (2021).
21. J. Postat, R. Olekhnovitch, F. Lemaître, P. Bousso, A Metabolism-Based Quorum Sensing Mechanism Contributes to Termination of Inflammatory Responses. *Immunity* **49**, 654-665.e655 (2018).
22. S. Recalcati, R. Pometta, S. Levi, D. Conte, G. Cairo, Response of monocyte iron regulatory protein activity to inflammation: abnormal behavior in genetic hemochromatosis. *Blood* **91**, 2565-2572 (1998).
23. G. Cairo, R. Ronchi, S. Recalcati, A. Campanella, G. Minotti, Nitric oxide and peroxynitrite activate the iron regulatory protein-1 of J774A.1 macrophages by direct disassembly of the Fe-S cluster of cytoplasmic aconitase. *Biochemistry* **41**, 7435-7442 (2002).
24. S. Kim, P. Ponka, Nitric oxide-mediated modulation of iron regulatory proteins: implication for cellular iron homeostasis. *Blood cells, molecules & diseases* **29**, 400-410 (2002).
25. T. S. Koskenkorva-Frank, G. Weiss, W. H. Koppenol, S. Burckhardt, The complex interplay of iron metabolism, reactive oxygen species, and reactive nitrogen species: insights into the potential of various iron therapies to induce oxidative and nitrosative stress. *Free radical biology & medicine* **65**, 1174-1194 (2013).
26. L. Solomon *et al.*, The dextran sulphate sodium (DSS) model of colitis: an overview. *Comparative Clinical Pathology* **19**, 235-239 (2010).

27. D. Kontoyiannis, M. Pasparakis, T. T. Pizarro, F. Cominelli, G. Kollias, Impaired on/off regulation of TNF biosynthesis in mice lacking TNF AU-rich elements: implications for joint and gut-associated immunopathologies. *Immunity* **10**, 387-398 (1999).
28. K. Pantopoulos, Iron metabolism and the IRE/IRP regulatory system: an update. *Ann N Y Acad Sci* **1012**, 1-13 (2004).
29. T. A. Rouault, Post-transcriptional regulation of human iron metabolism by iron regulatory proteins. *Blood cells, molecules & diseases* **29**, 309-314 (2002).
30. G. J. Mahler, M. L. Shuler, R. P. Glahn, Characterization of Caco-2 and HT29-MTX cocultures in an in vitro digestion/cell culture model used to predict iron bioavailability. *J Nutr Biochem* **20**, 494-502 (2009).
31. F. Leonard, E. M. Collnot, C. M. Lehr, A three-dimensional coculture of enterocytes, monocytes and dendritic cells to model inflamed intestinal mucosa in vitro. *Molecular pharmaceutics* **7**, 2103-2119 (2010).
32. F. Antunes, F. Andrade, F. Araujo, D. Ferreira, B. Sarmento, Establishment of a triple co-culture in vitro cell models to study intestinal absorption of peptide drugs. *European journal of pharmaceutics and biopharmaceutics : official journal of Arbeitsgemeinschaft fur Pharmazeutische Verfahrenstechnik e.V* **83**, 427-435 (2013).
33. T. Tanoue, Y. Nishitani, K. Kanazawa, T. Hashimoto, M. Mizuno, In vitro model to estimate gut inflammation using co-cultured Caco-2 and RAW264.7 cells. *Biochem Biophys Res Commun* **374**, 565-569 (2008).
34. S. Lund *et al.*, The dynamics of the LPS triggered inflammatory response of murine microglia under different culture and in vivo conditions. *J Neuroimmunol* **180**, 71-87 (2006).
35. S. Hobbs, M. Reynoso, A. V. Geddis, A. Y. Mitrophanov, R. W. Matheny, Jr., LPS-stimulated NF-κB p65 dynamic response marks the initiation of TNF expression and transition to IL-10 expression in RAW 264.7 macrophages. *Physiol Rep* **6**, e13914 (2018).
36. H. Domscheit, M. A. Hegeman, N. Carvalho, P. M. Spieth, Molecular Dynamics of Lipopolysaccharide-Induced Lung Injury in Rodents. *Frontiers in physiology* **11**, 36 (2020).
37. N. K. Gray *et al.*, Recombinant iron-regulatory factor functions as an iron-responsive-element-binding protein, a translational repressor and an aconitase. A functional assay for translational repression and direct demonstration of the iron switch. *European journal of biochemistry / FEBS* **218**, 657-667 (1993).
38. C. Bouton, M. J. Chauveau, S. Lazereg, J. C. Drapier, Recycling of RNA binding iron regulatory protein 1 into an aconitase after nitric oxide removal depends on mitochondrial ATP. *The Journal of biological chemistry* **277**, 31220-31227 (2002).
39. G. M. Tannahill *et al.*, Succinate is an inflammatory signal that induces IL-1β through HIF-1α. *Nature* **496**, 238-242 (2013).
40. F. Canal, C. Fosset, M. J. Chauveau, J. C. Drapier, C. Bouton, Regulation of the cysteine desulfurase Nfs1 and the scaffold protein IscU in macrophages stimulated with interferon-gamma and lipopolysaccharide. *Arch Biochem Biophys* **465**, 282-292 (2007).
41. A. Giatromanolaki *et al.*, Hypoxia inducible factor 1alpha and 2alpha overexpression in inflammatory bowel disease. *J Clin Pathol* **56**, 209-213 (2003).
42. M. Mastrogiannaki, P. Matak, C. Peyssonnaux, The gut in iron homeostasis: role of HIF-2 under normal and pathological conditions. *Blood* **122**, 885-892 (2013).
43. S. Recalcati, D. Taramelli, D. Conte, G. Cairo, Nitric oxide-mediated induction of ferritin synthesis in J774 macrophages by inflammatory cytokines: role of selective iron regulatory protein-2 downregulation. *Blood* **91**, 1059-1066 (1998).
44. P. Ruscitti *et al.*, Pro-inflammatory properties of H-ferritin on human macrophages, ex vivo and in vitro observations. *Scientific reports* **10**, 12232 (2020).
45. T. S. Olson *et al.*, The primary defect in experimental ileitis originates from a nonhematopoietic source. *The Journal of experimental medicine* **203**, 541-552 (2006).
46. M. Roulis, M. Armaka, M. Manoloukos, M. Apostolaki, G. Kollias, Intestinal epithelial cells as producers but not targets of chronic TNF suffice to cause murine Crohn-like pathology. *Proceedings of the National Academy of Sciences of the United States of America* **108**, 5396-5401 (2011).
47. E. Y. Choi *et al.*, Iron chelator triggers inflammatory signals in human intestinal epithelial cells: involvement of p38 and extracellular signal-regulated kinase signaling pathways. *J Immunol* **172**, 7069-7077 (2004).
48. M. C. Ghosh *et al.*, Tempol-mediated activation of latent iron regulatory protein activity prevents symptoms of neurodegenerative disease in IRP2 knockout mice. *Proceedings of the National Academy of Sciences of the United States of America* **105**, 12028-12033 (2008).
49. R. Medzhitov, The spectrum of inflammatory responses. *Science (New York, N.Y* **374**, 1070-1075 (2021).
50. J. T. Chang, Pathophysiology of Inflammatory Bowel Diseases. *N Engl J Med* **383**, 2652-2664 (2020).

51. R. Meli *et al.*, High Fat Diet Induces Liver Steatosis and Early Dysregulation of Iron Metabolism in Rats. *PLoS One* **8**, e66570 (2013).
52. D. Rachmilewitz *et al.*, Enhanced colonic nitric oxide generation and nitric oxide synthase activity in ulcerative colitis and Crohn's disease. *Gut* **36**, 718-723 (1995).
53. W. H. Tong *et al.*, TLR-activated repression of Fe-S cluster biogenesis drives a metabolic shift and alters histone and tubulin acetylation. *Blood Adv* **2**, 1146-1156 (2018).
54. T. Saito *et al.*, Transcriptional regulation of endochondral ossification by HIF-2alpha during skeletal growth and osteoarthritis development. *Nature medicine* **16**, 678-686 (2010).
55. D. R. Richardson, H. C. Lok, The nitric oxide-iron interplay in mammalian cells: transport and storage of dinitrosyl iron complexes. *Biochimica et biophysica acta* **1780**, 638-651 (2008).
56. Y. M. Shah, T. Matsubara, S. Ito, S. H. Yim, F. J. Gonzalez, Intestinal hypoxia-inducible transcription factors are essential for iron absorption following iron deficiency. *Cell metabolism* **9**, 152-164 (2009).
57. M. Mastrogiannaki *et al.*, HIF-2alpha, but not HIF-1alpha, promotes iron absorption in mice. *J Clin Invest* **119**, 1159-1166 (2009).
58. T. Werner *et al.*, Intestinal epithelial cell proteome from wild-type and TNFDeltaARE/WT mice: effect of iron on the development of chronic ileitis. *Journal of proteome research* **8**, 3252-3264 (2009).
59. N. J. Bessman *et al.*, Dendritic cell-derived hepcidin sequesters iron from the microbiota to promote mucosal healing. *Science (New York, N.Y* **368**, 186-189 (2020).
60. N. K. Das *et al.*, Microbial Metabolite Signaling Is Required for Systemic Iron Homeostasis. *Cell metabolism* **31**, 115-130.e116 (2020).
61. R. S. Bruckner *et al.*, Transplantation of Human Intestine Into the Mouse: A Novel Platform for Study of Inflammatory Enterocutaneous Fistulas. *Journal of Crohn's & colitis* **13**, 798-806 (2019).
62. S. Kuno, H. Fujita, Y. K. Tanaka, Y. Ogra, K. Iwai, Iron-induced NCOA4 condensation regulates ferritin fate and iron homeostasis. *EMBO reports*, e54278 (2022).
63. T. Ohshima, H. Yamamoto, Y. Sakamaki, C. Saito, N. Mizushima, NCOA4 drives ferritin phase separation to facilitate macroferritinophagy and microferritinophagy. *J Cell Biol* **221**, (2022).
64. J. D. Mancias, X. Wang, S. P. Gygi, J. W. Harper, A. C. Kimmelman, Quantitative proteomics identifies NCOA4 as the cargo receptor mediating ferritinophagy. *Nature* **509**, 105-109 (2014).
65. R. R. Starzynski *et al.*, Down-regulation of iron regulatory protein 1 activities and expression in superoxide dismutase 1 knock-out mice is not associated with alterations in iron metabolism. *The Journal of biological chemistry* **280**, 4207-4212 (2005).
66. A. Weiss *et al.*, Orchestrated regulation of iron trafficking proteins in the kidney during iron overload facilitates systemic iron retention. *PLoS One* **13**, e0204471 (2018).
67. E. G. Meyron-Holtz *et al.*, Genetic ablations of iron regulatory proteins 1 and 2 reveal why iron regulatory protein 2 dominates iron homeostasis. *The EMBO journal* **23**, 386-395 (2004).
68. W. H. Tong, T. A. Rouault, Functions of mitochondrial ISCU and cytosolic ISCU in mammalian iron-sulfur cluster biogenesis and iron homeostasis. *Cell metabolism* **3**, 199-210 (2006).
69. K. A. Schafer *et al.*, Use of Severity Grades to Characterize Histopathologic Changes. *Toxicologic pathology* **46**, 256-265 (2018).
70. A. Nyska *et al.*, Quantitative evaluation of chlortoluran-induced splenic hemosiderosis by means of an image analyzer. *Vet Hum Toxicol* **31**, 218-221 (1989).

Acknowledgements: We like to thank Dr. T.A. Rouault (NICHD, NIH, Bethesda MD, USA) for providing the IRP1$^{-/-}$ mice, Dr. F. Cominelli (Case Western Reserve University, Cleveland, OH, USA) for initially providing the *Tnf*$^{\Delta ARE/+}$ mice, and Dr. G. Kollias (BSRC Alexander Fleming Athens University Medical School, Athens, Greece) for subsequently sharing with us the *Tnf*$^{\Delta ARE/+}$ mice. Drs. Dan Gelvan, Vasiliki Koliaraki, Benjamin Podbilewicz and Dan Cassel and many former and present lab members of the E.M-H. lab have critically read the manuscript and supported this project with their thoughts and discussions.

Funding: This study was supported by grants from the Israel Science Foundation (No.755/09), the Joint Canada-Israel Program of the Israel Science Foundation (No. 3549/19), the Israeli Ministry of Health (No. 2026203 and 3-15072), and the Israeli Ministry of Science and Technology (No. 3-13438) to E.G. M-H.

Author contributions:

Conceptualization: EGMH

Methodology: LF, SB, WZ, NGR, NG, AN, AZ, MW, RW

Investigation: LF, SB, WZ, WHT, KL, NGR, NG, AN, AZ, MW, RW

Visualization: LF, SB, WZ, AZ

Funding acquisition: EGMH, NGR

Project administration: EGMH, LF, SB

Supervision: EGMH

Writing – original draft: LF, SB, WHT, EGMH

Writing – review & editing: EGMH, LF, WHT, KL, NGR, NG

Competing interests: EGMH and LF are inventors on a Provisional Patent Application, "Model for Analyzing inflammation and uses", US Provisional Patent Application No. 633/38,64 related to this work filed jointly by the Technion on July 13, 2022. The remaining authors declare no competing interests.

Data and materials availability: All materials are available from the authors on reasonable request with materials transfer agreements (MTAs).

Supplementary Materials

Materials and Methods

Figs. S1 to S7

Tables S1 to S5

References (*66–70*)

Figure 1

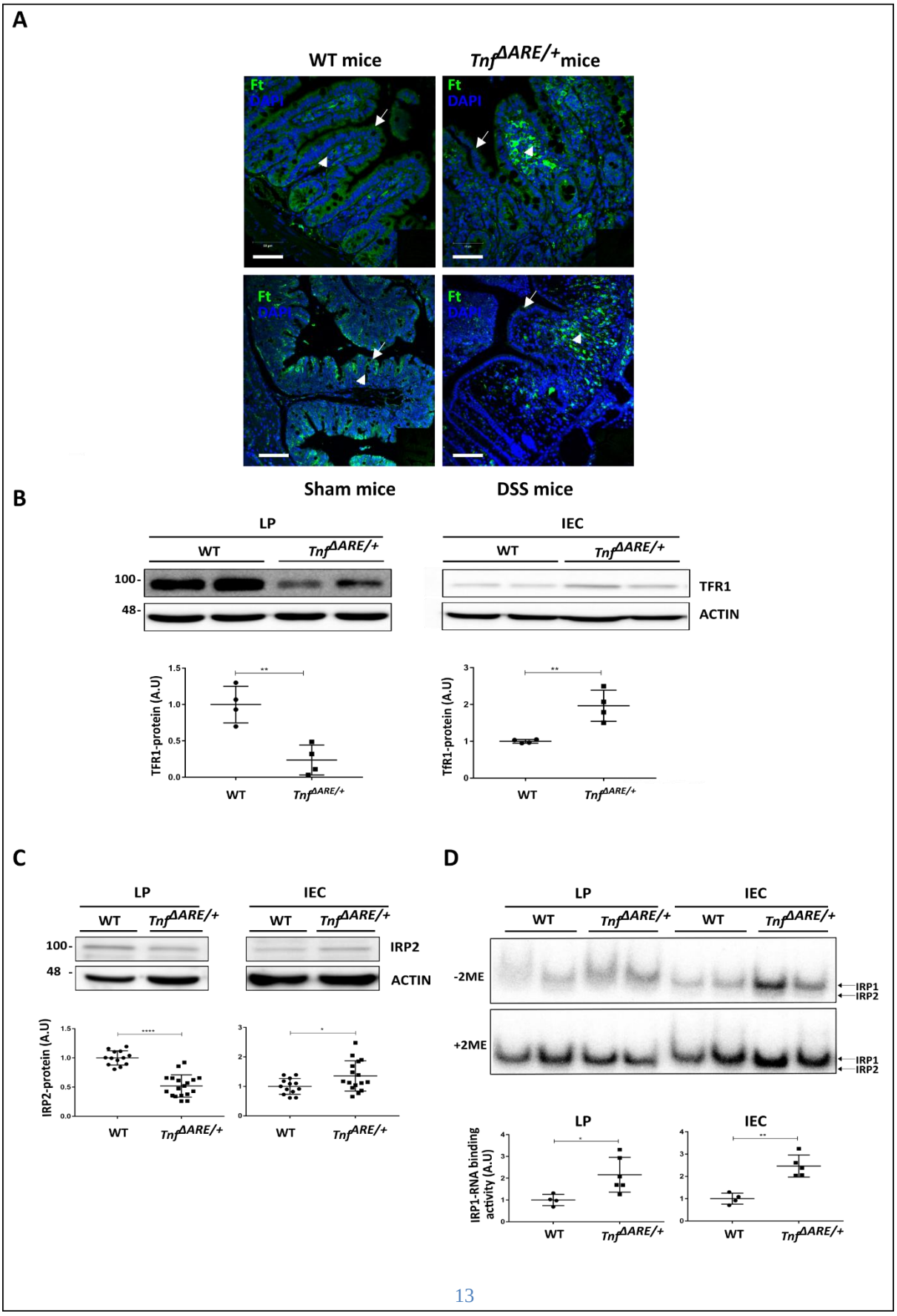
A
WT mice
Tnf ΔARE/+ mice
Ft
DAPI
B
Sham mice
DSS mice
LP
IEC
WT
Tnf ΔARE/+
100-
48-
TFR1
ACTIN
TFR1-protein (A.U)
TfR1-protein (A.U)
C
IRP2
IRP2-protein (A.U)
D
-2ME
+2ME
IRP1
IRP2
IRP1-RNA binding activity (A.U)

Figure 1: Inflammation drives a characteristic pattern of iron distribution. (**A**) Sections from terminal ileum (TI) of 12-14-week-old wild type (WT) and *Tnf*$^{\Delta ARE/+}$ mice on C57BL/6 background mice (n=3 each), or C57BL/6 mice exposed to 4% Dextran Sulfate Sodium (DSS) in their drinking water for 7 days, were immuno-stained for ferritin (green). Representative images show decreased ferritin levels in the inflamed intestinal epithelial cells (IEC) (arrows). Lamina propria (LP) cells show increased ferritin levels (arrow heads) in both inflammation models. Scale bars 50µm. **B-D** TI was harvested from 12-14 WT or *Tnf*$^{\Delta ARE/+}$ mice. IEC- and LP- enriched fractions were isolated and lysates further analyzed. Quantifications were done, using Image J. (**B)** Representative immuno-blot of Transferrin receptor-1 (TFR1) in LP and IEC fractions (mean ± SD (n=4)). TFR1 levels were decreased in the LP fraction of *Tnf*$^{\Delta ARE/+}$, compared to WT mice. **(C)** Representative immuno-blot of IRP2 in LP and IEC fractions (mean ± SD (n>16)). IRP2 levels were increased in IEC and decreased in LP fractions of the inflamed TI. (**D**) Representative radiograph of electromobility shift assay (EMSA) and quantification of IRP1-RNA-binding activity of the IEC and LP fractions of the TI. Addition of 2-mercaptoethanol (2-ME) to the lysate removes all Fe-S cluster from cAco/IRP1 and thus shows total IRP1-RNA-binding capacity. Values were normalized to +2-ME (mean ± SD (n>4)). IRP1 is activated in IEC and LP fractions of the inflamed TI of *Tnf*$^{\Delta ARE/+}$mice. IRP2 bands were detected just under the IRP1 band of the inflamed IEC fraction, consistent with the immunoblot data.

Figure 2

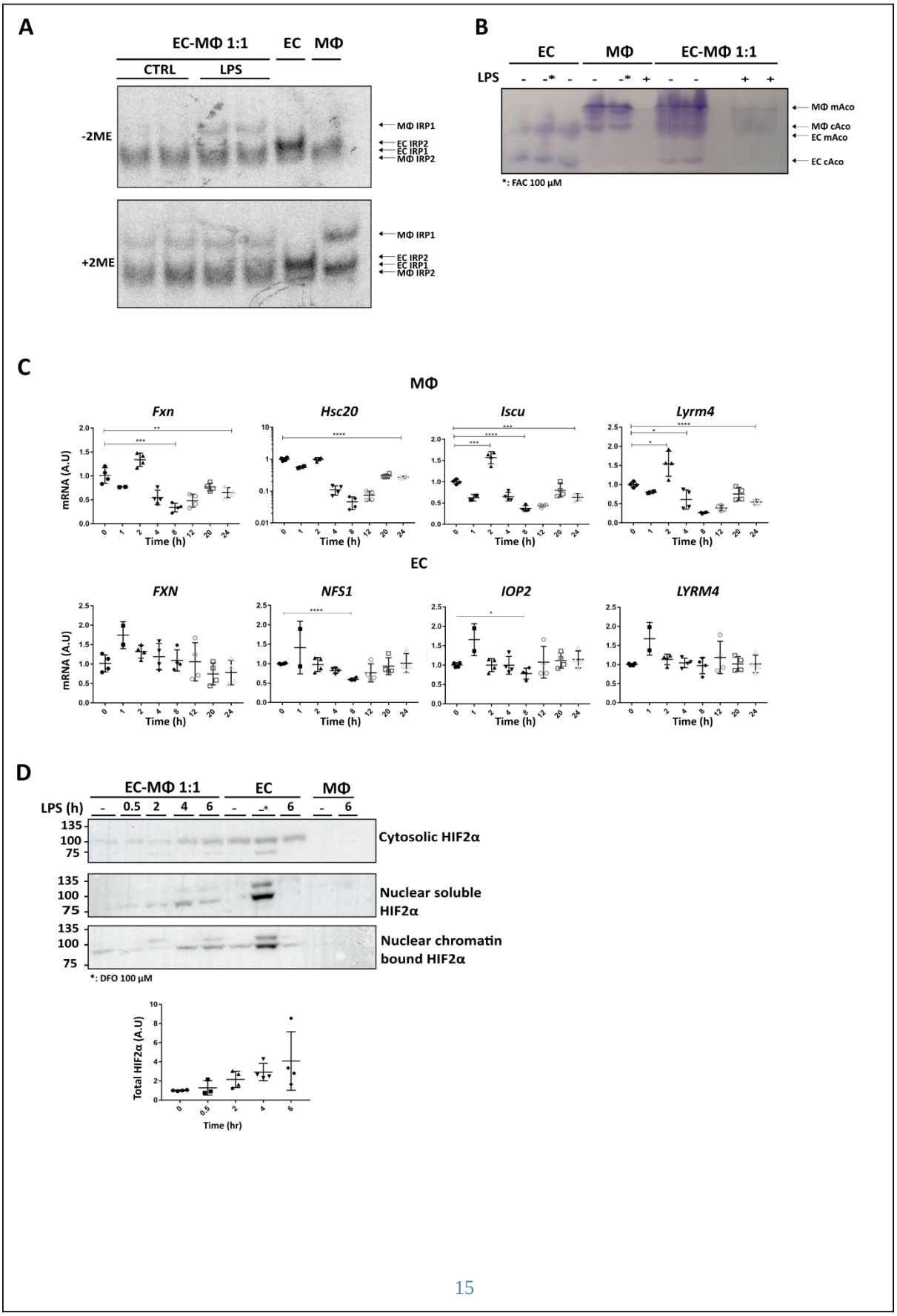
A
EC-MΦ 1:1
EC
MΦ
CTRL
LPS
-2ME
+2ME
MΦ IRP1
EC IRP2
EC IRP1
MΦ IRP2
B
EC
MΦ
EC-MΦ 1:1
LPS
MΦ mAco
MΦ cAco
EC mAco
EC cAco
*: FAC 100 µM
C
MΦ
Fxn
Hsc20
Iscu
Lyrm4
EC
FXN
NFS1
IOP2
LYRM4
mRNA (A.U)
Time (h)
D
EC-MΦ 1:1
EC
MΦ
LPS (h)
Cytosolic HIF2α
Nuclear soluble HIF2α
Nuclear chromatin bound HIF2α
*: DFO 100 µM
Total HIF2α (A.U)
Time (hr)

Figure 2: An interspecies co-culture model mimics the inflammation-associated activation of IRP1. Co-cultures of epithelial cells (EC) and macrophages (MΦ) were treated with 200 ng/ml LPS for 24 hr. Cells were harvested and lysed. (**A)** Lysates were subjected to EMSA for the detection of IRP-RNA (iron responsive element-IRE) binding activity (n= 4). Representative radiograph showing a significant increase in MΦ IRP1 RNA-binding activity upon LPS treatment. (**B)** Lysates were subjected to In-gel aconitase assay (n= 4). Representative gel showing decreased cytosolic and mitochondrial aconitase activities in EC and MΦs, upon LPS treatment. **(C)** RNA expression levels of key proteins associated with iron-sulfur cluster biogenesis were measured by RT-qPCR. Expression decreased significantly in MΦs and did not change in ECs. (**D)** Representative immunoblots of lysates after subcellular fraction. Protein levels were quantified with Image J. Values presented as mean ± SD (n=4). * 100 µM Desferrioxamine (DFO) for 24 hr. HIF2α levels increased significantly in ECs of LPS-stimulated co-cultures. In co-cultures, EC are always Caco2 cells. MΦs are as follows: Raw264.7 in **A, B** and **D**, and BMDM in **C**.

Figure 3

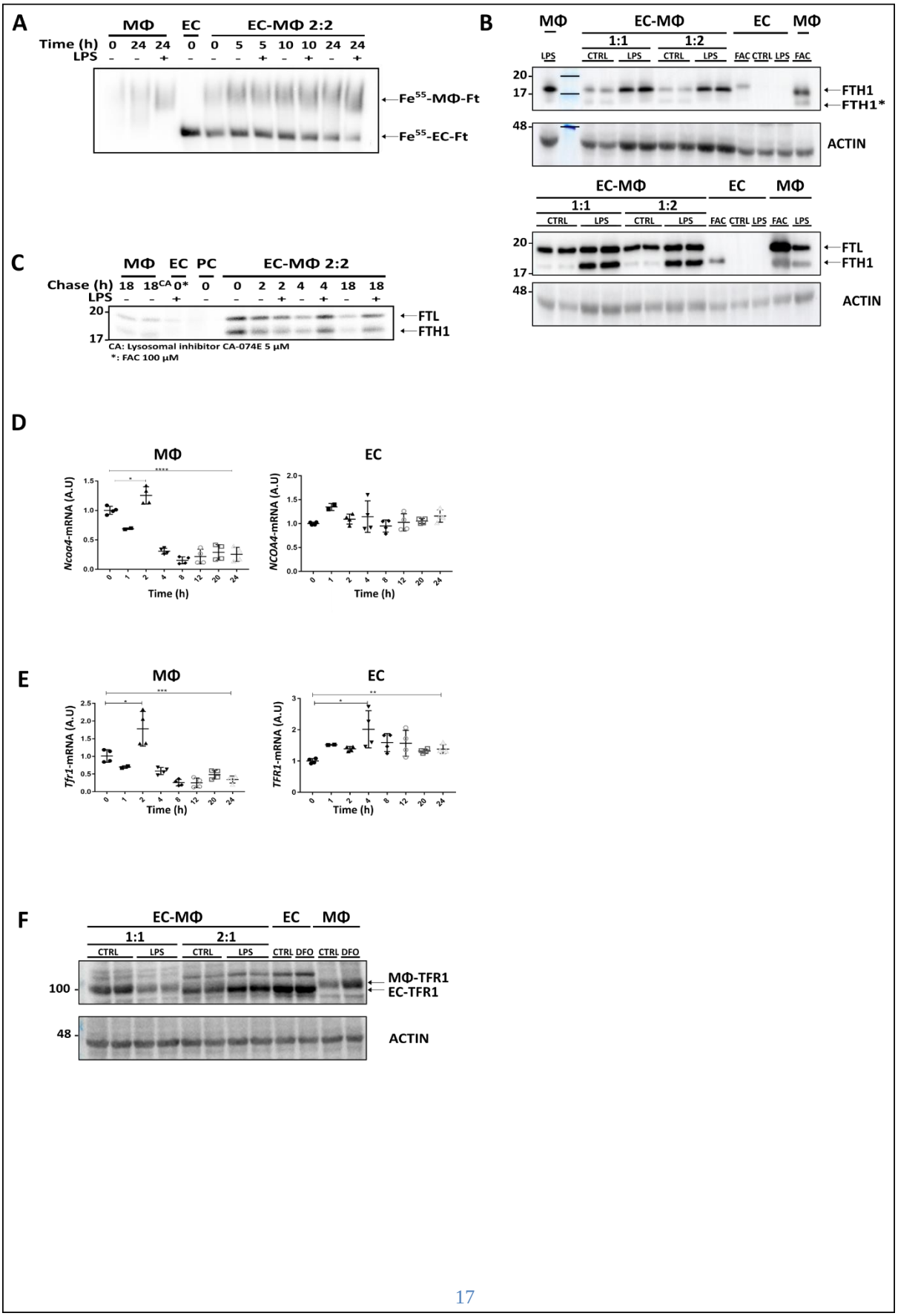
A
MΦ
EC
EC-MΦ 2:2
Time (h) 0 24 24 0 0 5 5 10 10 24 24
LPS - - + - - - + - + - +
Fe55-MΦ-Ft
Fe55-EC-Ft
B
MΦ
EC-MΦ
EC
MΦ
1:1
1:2
LPS
CTRL LPS CTRL LPS FAC CTRL LPS FAC
20
17
48
FTH1
FTH1*
ACTIN
EC-MΦ
EC
MΦ
1:1
1:2
CTRL LPS CTRL LPS FAC CTRL LPS FAC LPS
20
17
48
FTL
FTH1
ACTIN
C
MΦ EC PC EC-MΦ 2:2
Chase (h) 18 18CA 0* 0 0 2 2 4 4 18 18
LPS - - + - - - + - + - +
20
17
FTL
FTH1
CA: Lysosomal inhibitor CA-074E 5 µM
*: FAC 100 µM
D
MΦ
EC
Ncoa4-mRNA (A.U)
NCOA4-mRNA (A.U)
Time (h)
E
MΦ
EC
Tfr1-mRNA (A.U)
TFR1-mRNA (A.U)
Time (h)
F
EC-MΦ
EC
MΦ
1:1
2:1
CTRL LPS CTRL LPS CTRL DFO CTRL DFO
100
48
MΦ-TFR1
EC-TFR1
ACTIN

Figure 3: Iron-regulated proteins sense the inflammatory iron state of reduced epithelial and increased macrophage iron and respond accordingly. Co-cultures of epithelial cells (EC) and macrophages (MΦ) were treated with 200 ng/ml LPS as indicated. **(A)** Co-cultures were pretreated with ^{55}Fe-labeled human transferrin for 16 hr, washed and treated with LPS as indicated. Cell-lysates were separated on a native gel (n=2). Representative radiograph shows increased ferritin-iron in MΦs and decreased ferritin-iron in epithelial cells 24 hr after LPS stimulation. (**B)** Representative immunoblot of the ferritin H-subunit (FtH) and ferritin L-subunit (FtL). EC ferritin was not detected (except in FAC treated ECs), thus the bands are MΦ ferritin only. Anti-FtL antibody detects both subunits (FtH is the lower band just above the 17kD Mw-marker) n=2. MΦ Ft-H was significantly increased, and the FtH degradation product (*FtH) decreased after LPS stimulation. (**C)** Metabolic labeling (^{35}S) pulse-chase experiment of LPS-stimulated EC-MΦ (BMDM) co-cultures as indicated, followed by ferritin immunoprecipitation (IP) (n=2). MΦ ferritin undergoes less degradation following LPS stimulation. (**D)** RNA expression levels of *Ncoa4* were measured in co-cultures by RT-qPCR (n=4). Levels of *Ncoa4* were significantly decreased in inflamed MΦs, but not in ECs. Co-cultures were treated with 200 ng/ml LPS for indicated times **E** and 24 hr **F. (E)** Transferrin receptor-1 (*Tfr1*) RNA expression levels were measured by RT-qPCR (n=4). *Tfr1* expression levels showed dynamic changes throughout the course of LPS stimulation and were decreased in MΦs and increased in ECs at the 24 hr time point. (**F)** Representative immunoblot of TFR1 (n=12). Tfr1 levels were decreased in MΦs (visible strongly in co-cultures grown at 1:1 EC:MΦ ratio, as in these conditions the Raw 264.7 cells that proliferate faster than Caco2 cells are the dominating cells) and increased in ECs (visible strongly in co-cultures grown at 2:1 EC:MΦ ratio, where ECs remain dominant and a faint murine Tfr1 band is visible above the human TFR1). In co-cultures, EC are always Caco2 cells. MΦs are as follows: BMDM in **A – E**, and Raw264.7 in **F**.

Figure 4

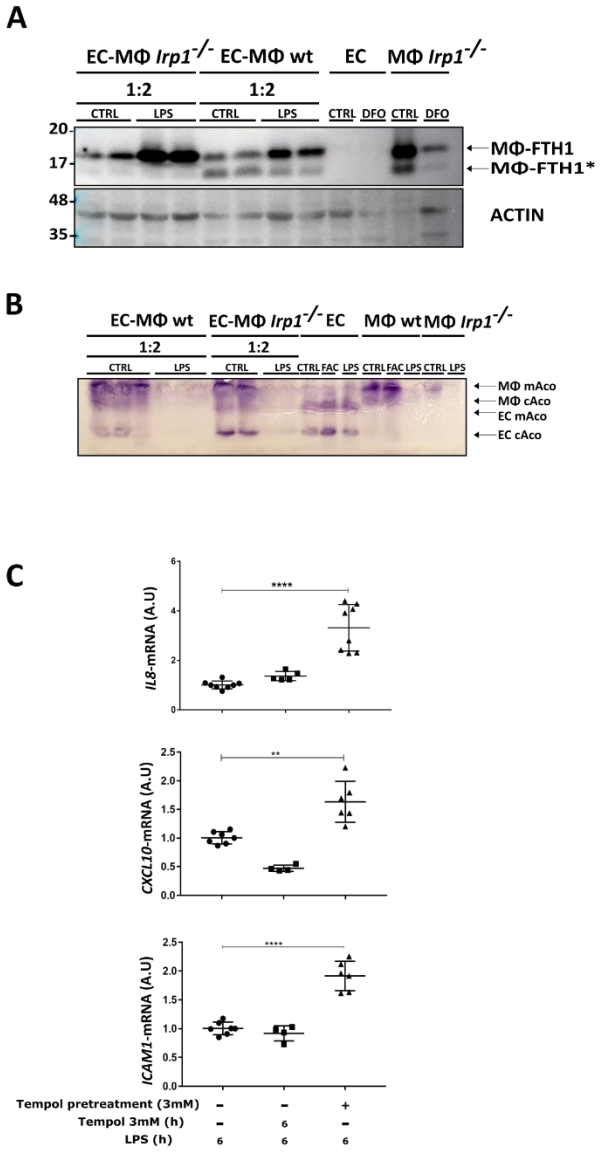
A
EC-MΦ Irp1-/-
EC-MΦ wt
EC
MΦ Irp1-/-
1:2
1:2
CTRL
LPS
CTRL
LPS
CTRL
DFO
CTRL
DFO
20
17
48
35
MΦ-FTH1
MΦ-FTH1*
ACTIN
B
EC-MΦ wt
EC-MΦ Irp1-/-
EC
MΦ wt
MΦ Irp1-/-
1:2
1:2
CTRL
LPS
CTRL
LPS
CTRL
FAC
LPS
CTRL
FAC
LPS
CTRL
LPS
MΦ mAco
MΦ cAco
EC mAco
EC cAco
C
IL8-mRNA (A.U)
****
CXCL10-mRNA (A.U)
**
ICAM1-mRNA (A.U)
****
Tempol pretreatment (3mM)
Tempol 3mM (h)
LPS (h)

Figure 4: Macrophage and epithelial IRP1-IRE-binding-activity play different roles in intestinal inflammation. (A) Co-cultures of EC with *wt*-BMDM or with BMDM with targeted deletion of IRP1 (MΦ *Irp1*$^{-/-}$) were stimulated with 200 ng/ml LPS for 24 hr. Co-culture of EC-MΦ *Irp1*$^{-/-}$ did not restore iron homeostasis upon LPS stimulation. Representative immunoblot of FtH (*FtH-degradation product) (n=8). MΦ FtH was significantly increased in both EC-MΦ*wt* and EC-MΦ*Irp1*$^{-/-}$ co-cultures upon LPS stimulation. **(B)** In-gel aconitase assay (n= 4). Representative gel showing decreased cytosolic and mitochondrial aconitase activities in EC-MΦ *wt* and EC-MΦ *Irp1*$^{-/-}$ co-cultures, upon LPS treatment. (**C)** ECs (Caco2) were pretreated with 3mM tempol for 16 hr, washed, and then co-cultured with MΦs (Raw 264.7). After MΦs adhered, LPS and/or tempol was added for 6 hr as indicated. RNA expression levels were measured by RT-qPCR (n=6). Pre-treatment of ECs with tempol significantly increased the expression levels of selected epithelial pro-inflammatory markers, compared to LPS-only stimulated co-cultures.

Figure 5

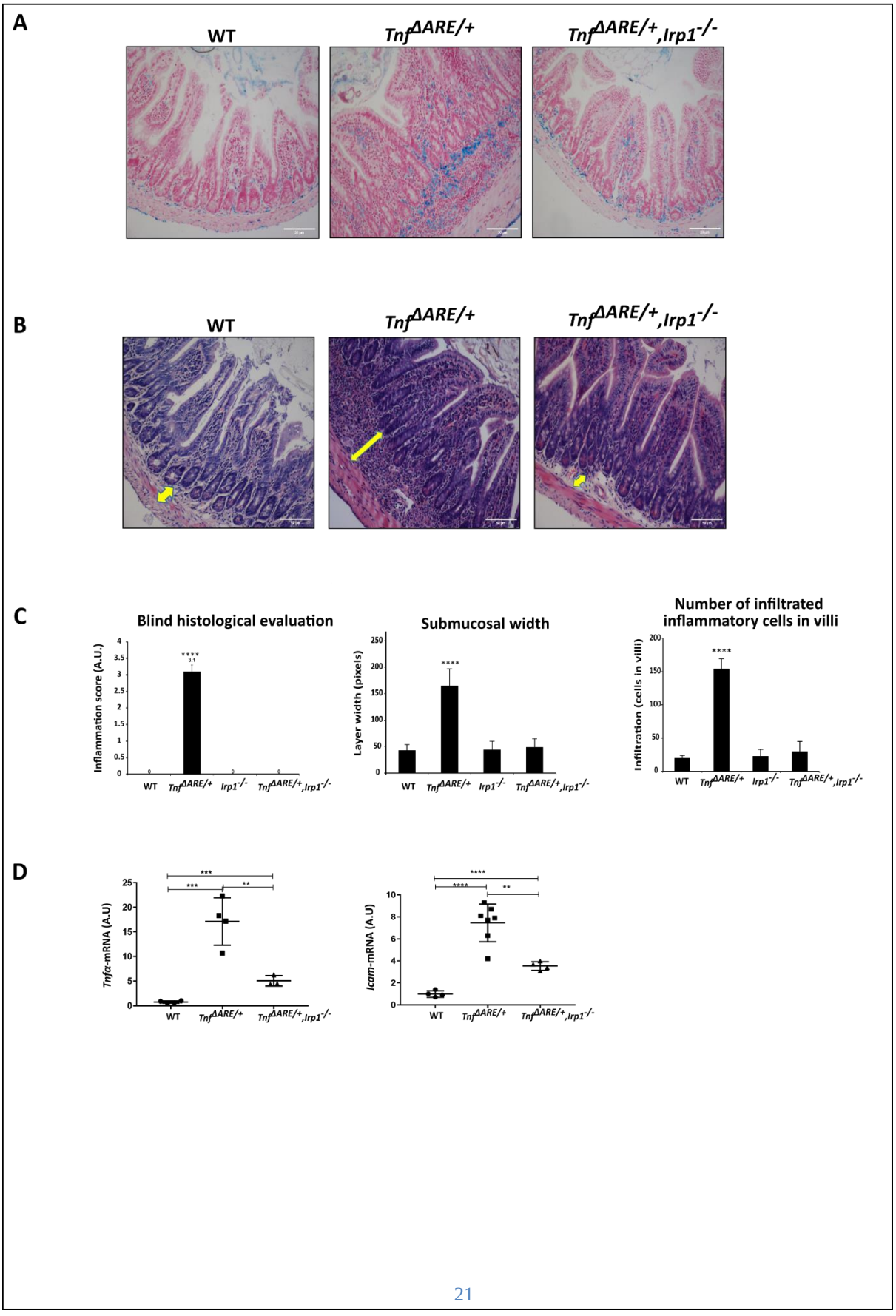
A
WT
Tnf ΔARE/+
Tnf ΔARE/+,Irp1 -/-
B
WT
Tnf ΔARE/+
Tnf ΔARE/+,Irp1 -/-
C
Blind histological evaluation
Inflammation score (A.U.)
Submucosal width
Layer width (pixels)
Number of infiltrated inflammatory cells in villi
Infiltration (cells in villi)
WT
Tnf ΔARE/+
Irp1 -/-
Tnf ΔARE/+,Irp1 -/-
D
Tnfα-mRNA (A.U)
Icam-mRNA (A.U)

Figure 5: Deletion of IRP1 restores iron homeostasis and inhibits the inflammatory process in the *Tnf*$^{\Delta ARE/+}$ mouse model. (A) Representative image of terminal ileum (TI) section of iron-overloaded mice stained with Perls stain. (**B)** Representative hematoxylin and eosin-stained TI sections illustrating normal histology in *Tnf*$^{\Delta ARE/+}$, *Irp1*$^{-/-}$ mice, compared to *Tnf*$^{\Delta ARE/+}$ mice. The arrows highlight the width of the submucosal layer. **(C)** Blind histological evaluations (n= 6). (**D)** RNA expression levels of selected proinflammatory cytokines were measured by RT-qPCR (n=4-7) and were significantly decreased in the TI of *Tnf*$^{\Delta ARE/+}$, *Irp1*$^{-/-}$ mice, compared to *Tnf*$^{\Delta ARE/+}$mice.

Figure 6

A

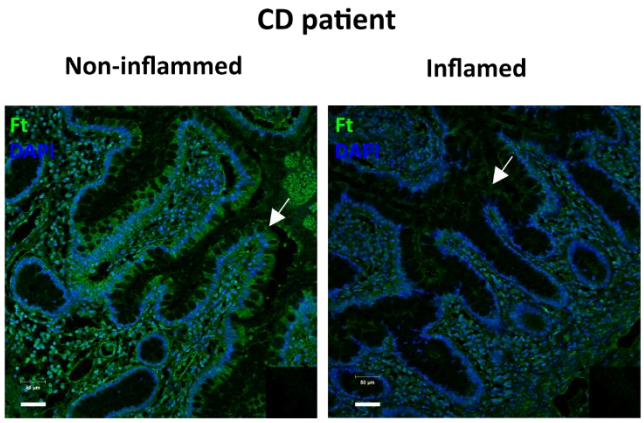
CD patient
Non-inflammed
Inflamed
Ft
DAPI
Ft
DAPI

B

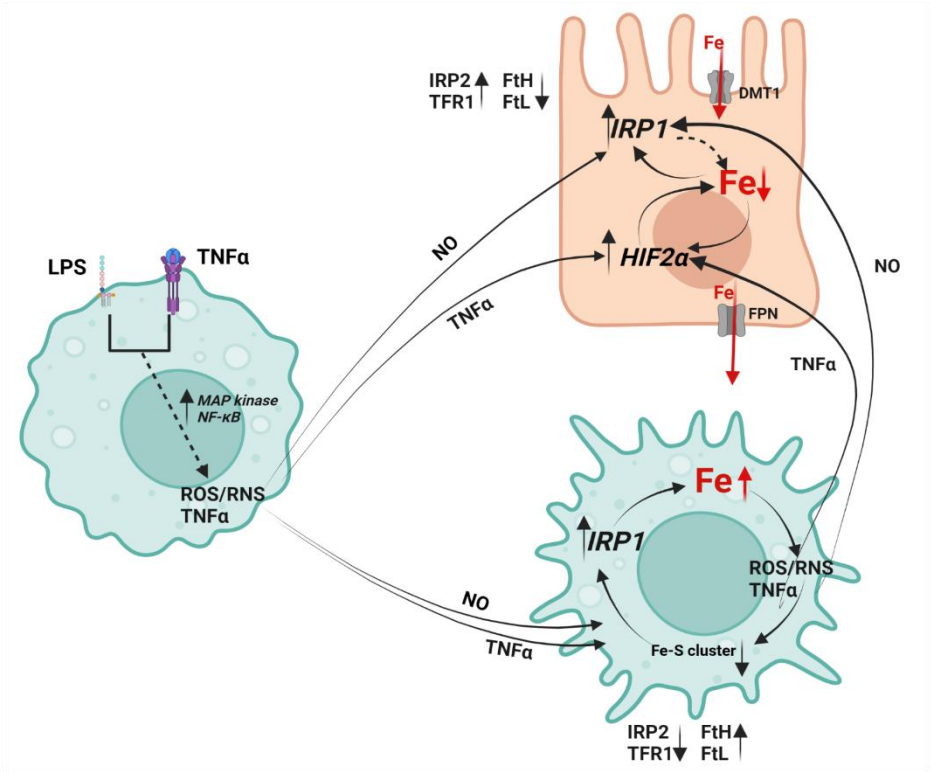
IRP2 ↑ FtH ↓
TFR1 ↑ FtL ↓
Fe
DMT1
IRP1
Fe↓
HIF2α
Fe
FPN
NO
NO
TNFα
TNFα
LPS
TNFα
MAP kinase
NF-κB
ROS/RNS
TNFα
Fe↑
IRP1
ROS/RNS
TNFα
NO
TNFα
Fe-S cluster
IRP2 ↓ FtH ↑
TFR1 ↓ FtL ↑

Figure 6: Modified iron homeostasis is observed in the inflamed lesions of CD patients

(A) Sections from non-inflamed and inflamed intestinal areas of Crohn's disease patients (n=8) were immuno-stained for ferritin (green). Representative images show that the inflamed epithelial cells (IEC) (arrows) have decreased ferritin levels. Scale bars 50µm. (**B)** A schematic presentation of the involvement of IRP1 in the self-accelerating inflammatory process. Description. Macrophages activated to a proinflammatory response secrete nitric oxide (NO) and proinflammatory cytokines, such as Tnfα to their immediate environment, both reaching neighboring cells, including epithelial cells. In epithelial cells, Tnfα activates the hypoxia inducible factor HIF2α, which mediates increased iron flux from the intestinal lumen to the lamina propria and NO activates IRP1, which inhibits ferritin translation and thus inhibits ferritin storage, which further increases the iron flux. In macrophages NO activates IRP1 and thus maintains a certain level of increased iron influx that continues to promote iron overload, which supports the pro-inflammatory polarization of the macrophage. The inflammation-mediated reduction of iron sulfur cluster assembly in macrophages and increase of HIF2α in epithelial cells continue to support the activity of IRP1 and the iron flux from epithelial cells to macrophages, which maintains the inflammatory iron pattern and perpetuates the inflammation.